ORNL-Sub-3649-2

The Effect of Biaxiality in Creep-Fatigue at Elevated Temperatures

Annual Report

January 1, 1973 to December 31, 1973

S. Y. Zamrik

Department of Engineering Mechanics
The Pennsylvania State University
University Park, Pennsylvania

Prepared for

Oak Ridge National Laboratory
Operated by Union Carbide Corporation
For the U.S. Atomic Energy Commission
Under Contract No. 3649

Table of Contents

List of Illustrations

List of Tables

Abstract

The effect of biaxiality in creep-fatigue interaction at elevated temperature is being investigated. Biaxial fatigue tests were conducted with thin-walled tubular specimens loaded with axial tension-compression and torsion. Biaxial strains were imposed under synchronous loading condition at 25 cycles per minute. Specimens were obtained from extruded 304 stainless steel rods, machined to specifications and annealed in an argon atmosphere at 1092°C (2000°F).

The experimental data covers biaxial fatigue tests at room, 1000°F and 1200°F, biaxial cumulative fatigue damage tests under a high to low loading sequence at 1000°F and 1200°F, and tensile properties tests at 900°F to 1200°F.

Introduction

The objective of the present research program, sponsored by Oak Ridge National Laboratory, Union Carbide Corporation under Contract No. 3649, is to evaluate, experimentally, the effect of elevated temperature environment on fatigue failure of type 304 stainless steel under biaxial stress condition. The program will also develop an evaluation of current design criteria for biaxial fatigue analysis, biaxial cumulative fatigue damage and creep effect as a result of hold-time under biaxial cycling conditions. The reported data is analyzed on the basis of the present yield criterion of the octahedral shear strain range theory. In this respect, it will provide designers with a general view of the limitations of adopting such criteria in the presence of elevated temperatures. Interpretations of the data are not forwarded in this report since the comprehensive goals of this research effort have not been completed; however, some conclusions and trends can be drawn as a tentative guide for the purpose of preliminary analysis. An environment of 1200°F has a greater damaging effect on the biaxial fatigue and cumulative damage of the 304 stainless steel material than a 1000°F.

Although the experimental procedure has been reported previously, its repetition will provide a comprehensive view of the technique used to obtain the data.

Experimental Procedure

1. Material Tested and Specimens

The material used in this investigation is 304 stainless steel (ORNL heat number 9T2796) extruded in rod form with a one inch diameter. Specimens were machined and honed according to the specifications shown in Figure (1), then annealed at 1092°C for 30 minutes in an argon atmosphere.

A chart (Table 6) was prepared for each received rod showing the location of the specimen tested.

2. Test Equipment

The biaxial fatigue machine is a servo-controlled electro hydraulic system operated in a closed loop strain or load control. The equipment is capable of imposing axial and torsional strain on a specimen in a synchronous or nonsynchronous (out-of-phase) loading. The out-of-phase strain capability ranges from 0 through 180°. In the in-phase cycling, various types of loading functions can be imposed at fixed or variable frequencies. Figure (2) shows the closed loop loading system used in this program.

The temperature was imposed on the specimen through glo-bar heating elements manufactured by the Carborundum Corporation. The element, 6 1/2 inches long with 1/4 inch diameter, is of silicon carbide with a central heating section or "hot zone" that varies from 1-1/2 inches to 2 inches long. The element was inserted in the tubular specimen and left free to expand or contract. Electrical connection was made through the aluminum metallized terminals. Figure (3) shows the heating element inserted in the specimen. Because of the high temperature environment, the strain was controlled through an LVDT extensometer for the axial strain and through an

HIGH-TEMP. FATIGUE SPECIMEN

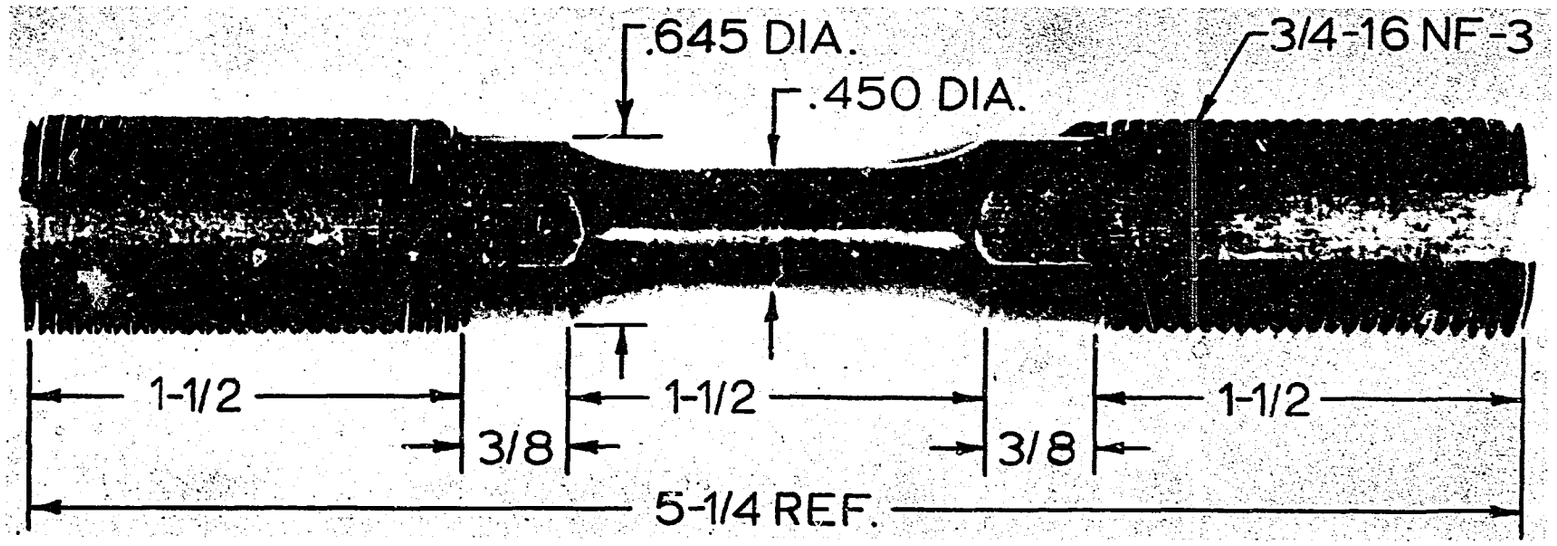

NOTES: GROOVES ARE .250 WIDE X .062 DEEP
FILLET RADIUS IS 3/4
.060 WALL THICKNESS OVER GAGE LENGTH

Figure 1

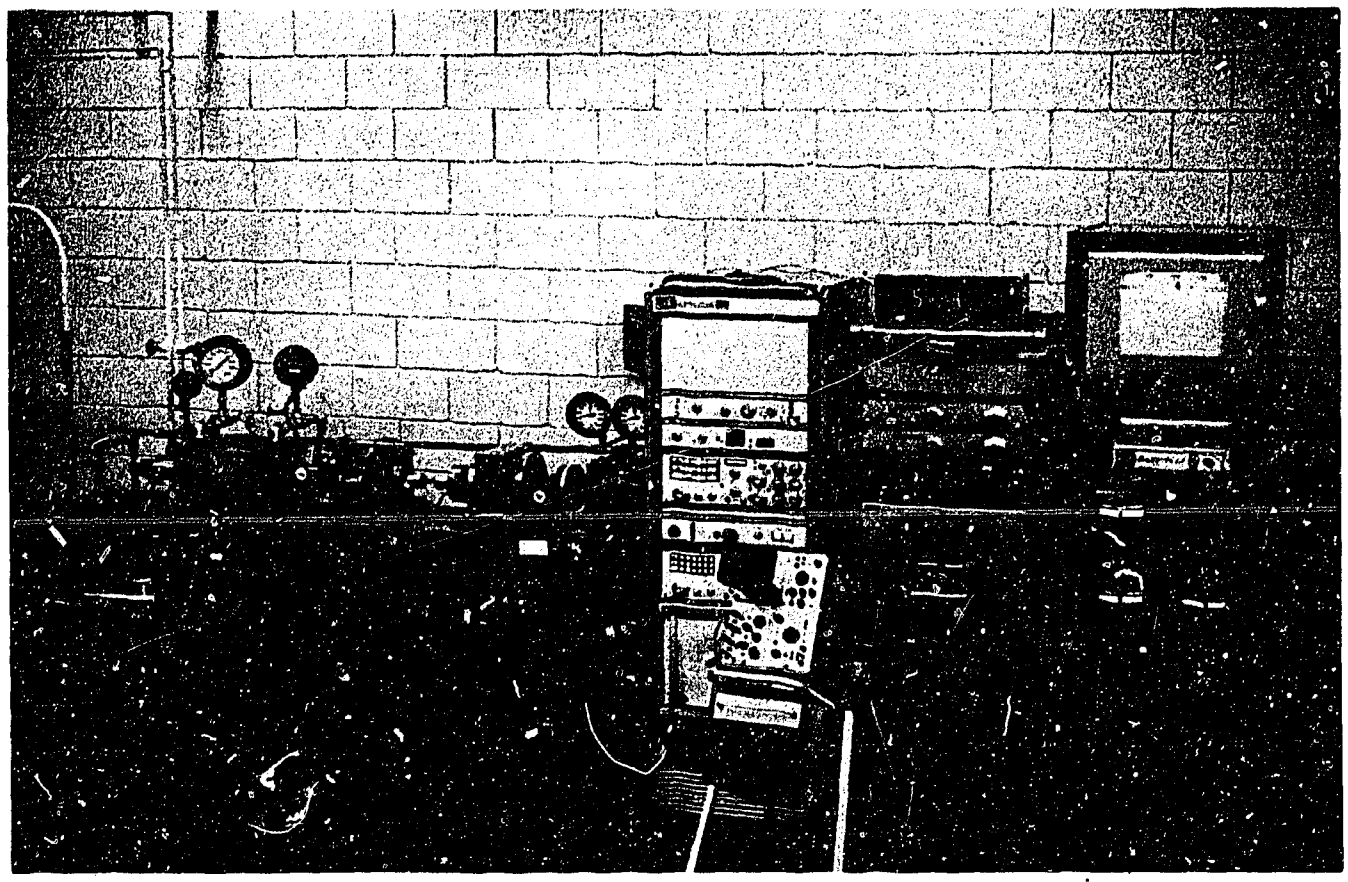

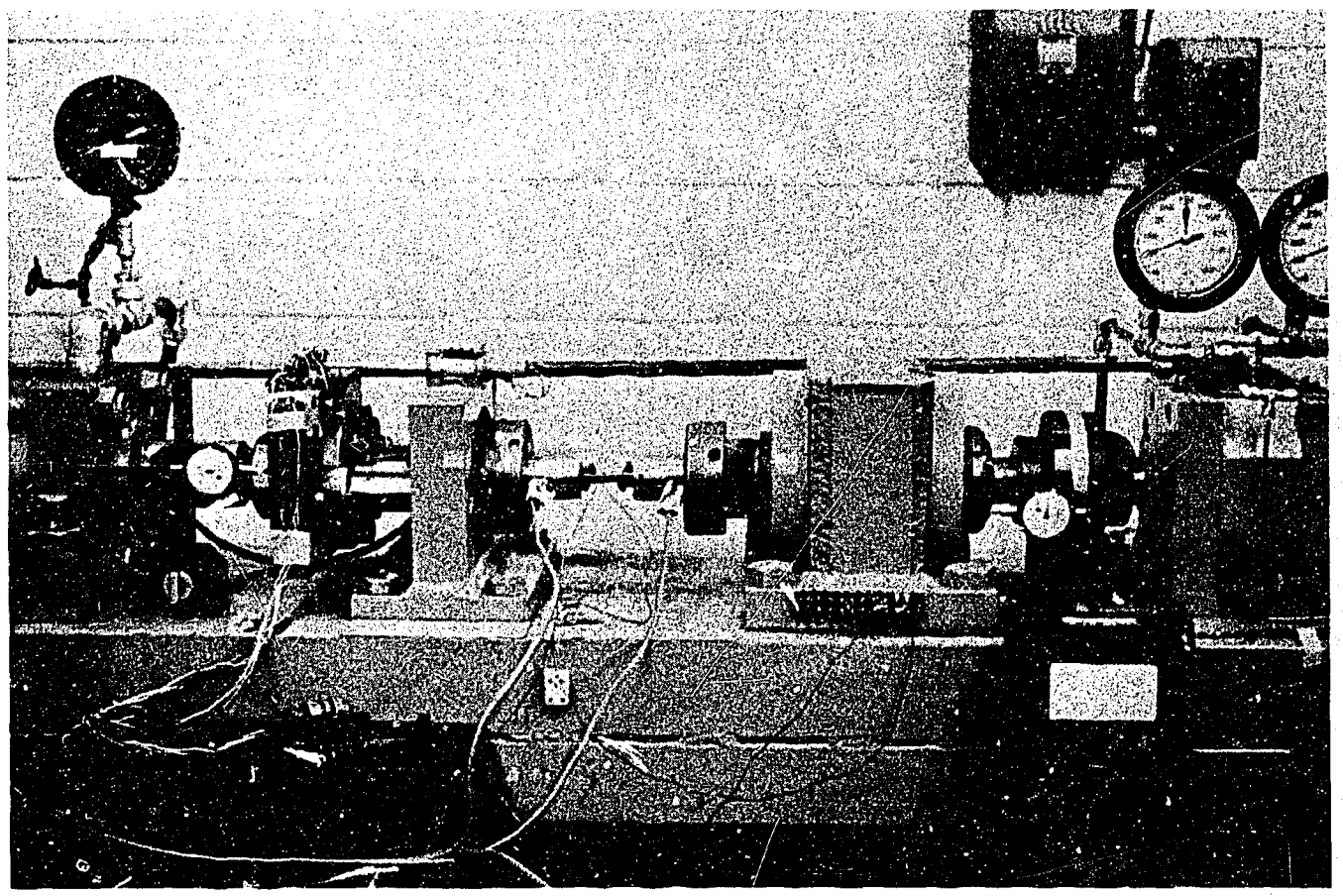

Figure 2. Biaxial strain cycling fatigue machine. (a) General layout of equipment. (b) Specimen attachment and measuring devices.

HIGH-TEMP. FATIGUE SPECIMEN

FULL SECTIONAL VIEW SHOWING HEATING ELEMENT

Figure 3

RVDT extensometer for the torsional strain. Both extensometers were calibrated with a load cell mounted in the arm of the axial loading ramp.

The combined strains were imposed on the specimen as shown in Figure (4) at 25 cycles per minute. Strain measurements were carried out at room temperature by placing high-elongation strain gages on the specimen surface in a rosette type and then correlated with the axial and torsional extensometers.

Fatigue Data and Analysis

The data presented in this report covers biaxial fatigue tests at 1000°F and 1200°F, biaxial cumulative fatigue damage tests at 1200°F and tensile properties tests at temperatures of 900 to 1200°F.

1. Biaxial Fatigue Tests

Thin-walled tubular specimens of 304 stainless steel were subjected to strain ratios of torsional shear strain range, $\Delta\gamma_{x\theta}$, to axial strain range, $\Delta\varepsilon_x$, of 0.5, 1.0, 2.0, and 5.0. Both types of strains were imposed simultaneously in a completely reversible and sinusoidal loading.

In the analysis of the data, the current design criteria of the maximum principal strain range, $\Delta\varepsilon_1$, the effective strain range, $\Delta\bar{\varepsilon}_e$, and the octahedral shear strain range, $\Delta\gamma_{oct}$, can all be interrelated if one assumes the volume to remain constant in the low cycle fatigue region. In this case, the assumption of Poisson's ratio of 1/2 is valid, hence:

$$\Delta\varepsilon_1 + \Delta\varepsilon_2 + \Delta\varepsilon_3 = 0 \qquad (1)$$

Expressing the octahedral shear strain, γ, as:

$$\gamma = \frac{2}{3}\sqrt{(\varepsilon_1 - \varepsilon_2)^2 + (\varepsilon_2 - \varepsilon_3)^2 + (\varepsilon_3 - \varepsilon_1)^2} \qquad (2)$$

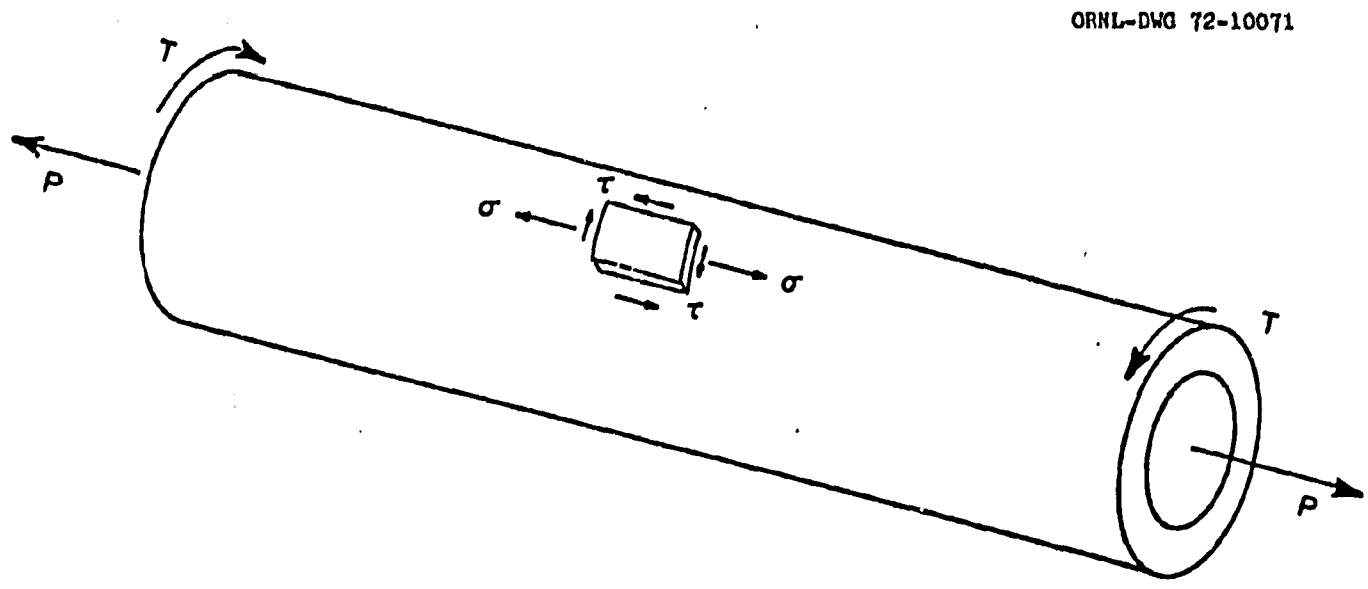

Fig. 4 Tubular specimen and surface element — biaxial loading system.

Then the three criteria are related in the form:

$$\Delta\gamma_{oct} = \sqrt{2}\,\Delta\bar{\varepsilon}_e \tag{3}$$

and

$$\Delta\bar{\varepsilon}_e = \frac{2}{\sqrt{3}}\,\Delta\varepsilon_1\sqrt{1 + \phi + \phi^2} \tag{4}$$

or in terms of the applied strains:

$$\Delta\bar{\varepsilon}_e = \frac{2}{\sqrt{3}}\left[\frac{\Delta\varepsilon_1}{0.5 + \sqrt{2.25 + R^2}}\right][3 + R^2]^{1/2} \tag{5}$$

where $\phi = \Delta\varepsilon_2/\Delta\varepsilon_1$ and $R = \Delta\gamma_{x\theta}/\Delta\varepsilon_x$.

The interrelation between the three concepts is a constant. This can be observed in examining Tables (1) and (2), where, for example, the deviation of $\Delta\bar{\varepsilon}_e$ as compared to $\Delta\varepsilon_1$ for R = 0 to R = 4 is negligible (Table 2).

To simplify the evaluation of data obtained thus far for room 1000°F and 1200°F temperatures under axial, torsional, and biaxial tests, the octahedral shear strain range will be used as a reference. Thus, the converted data of all tests is shown in Figures (5), (6), and (7).

In Figure (5), the upper bound represents the pure torsional data and the lower bound represents the axial data. The biaxial data varies between the two bounds, for example, the biaxial tests for a strain ratio of 0.5 fall along the axial data for low values of shear strain and approaches the upper bound of pure torsional data as the shear strain increases. The classical octahedral shear strain theory is used as an interpretative method to biaxial room temperature data. It is related to the number of cycles to failure in a power law relationship in the form of:

$$\Delta\gamma_{oct}N^{\alpha} = C \tag{6}$$

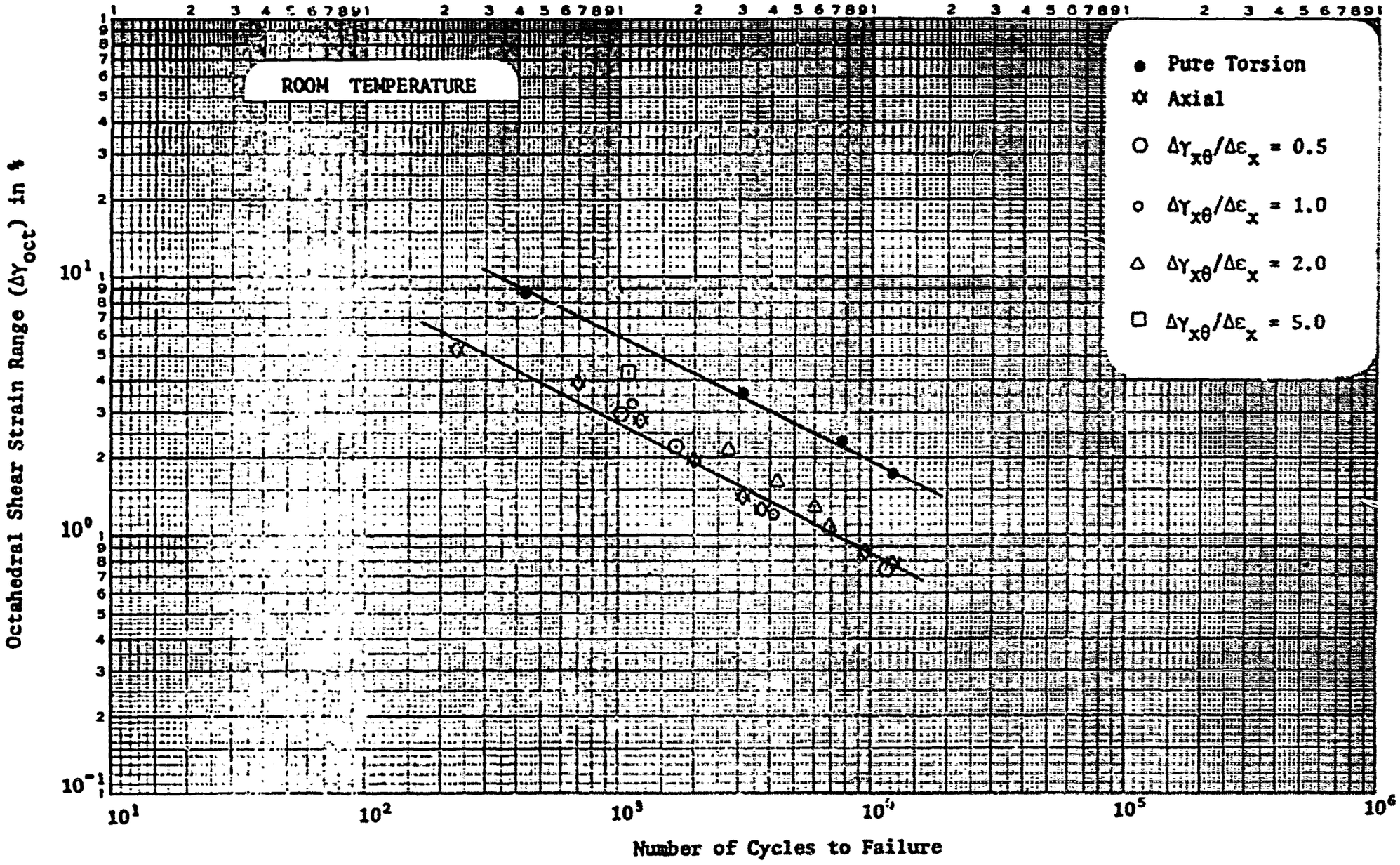

Figure 5. Comparison of Axial to Biaxial Fatigue Tests at Room Temperature

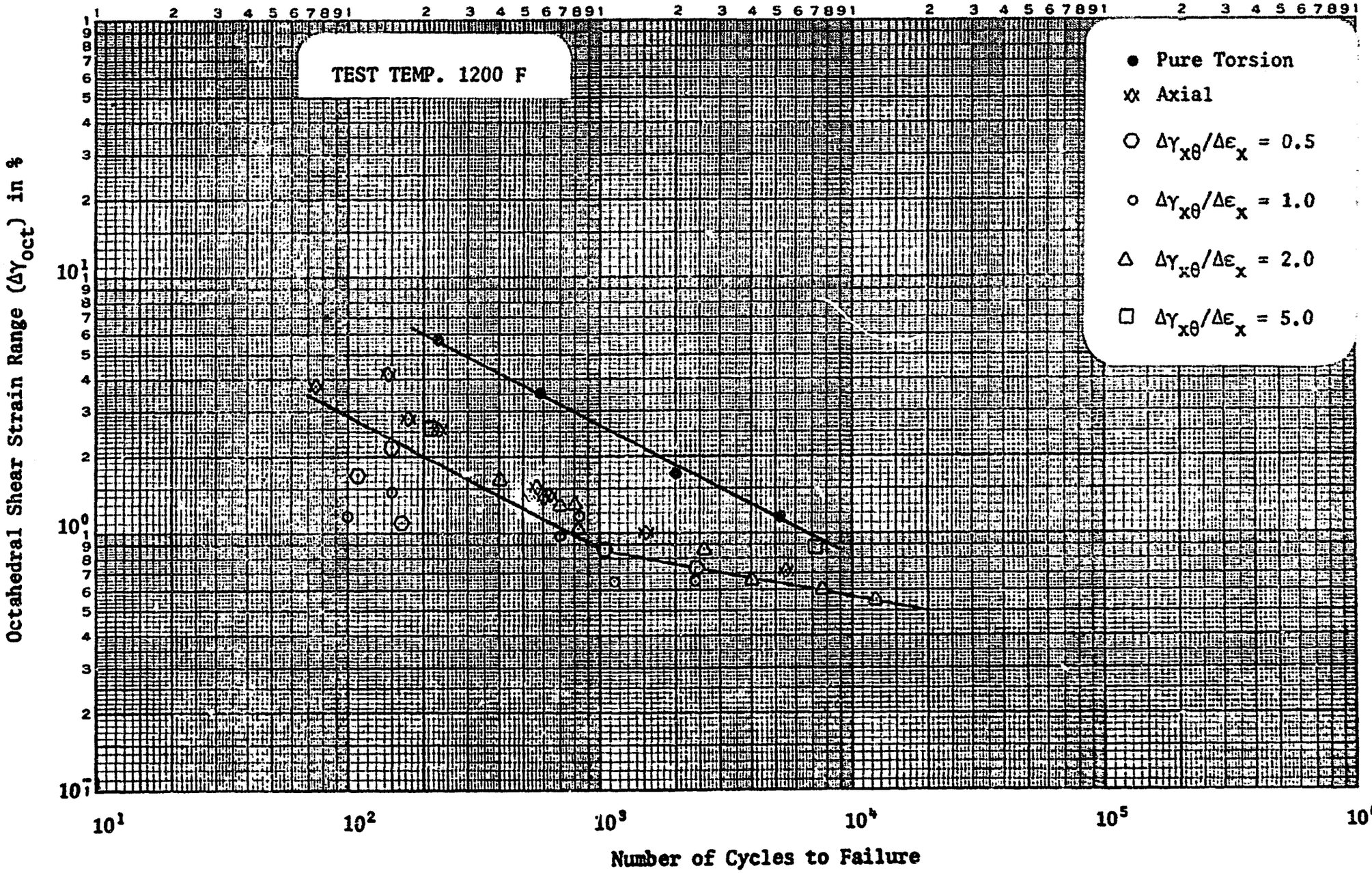

Figure 6. Comparison of Axial to Biaxial Fatigue Tests at 1200°F

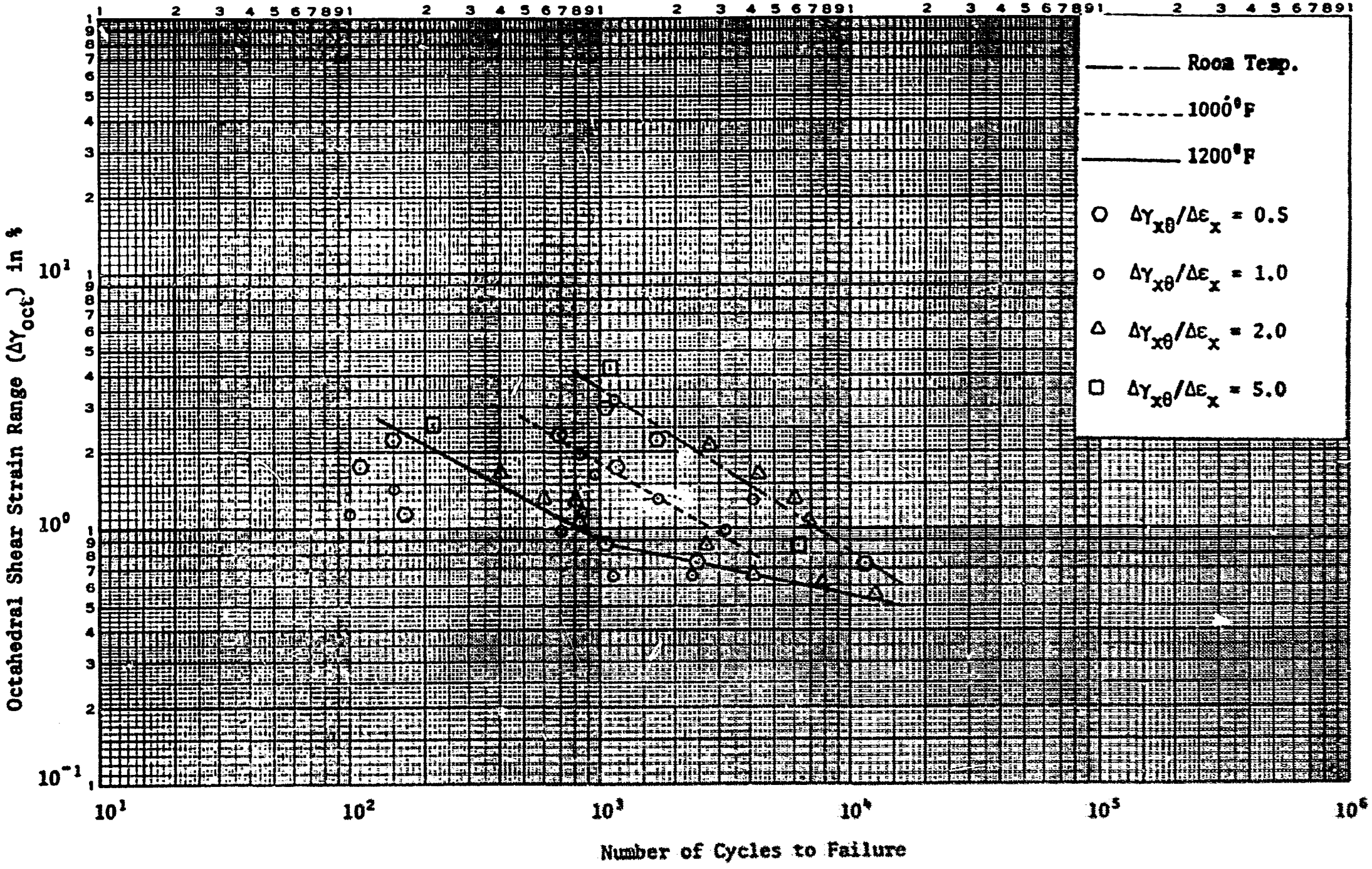

Figure 7. Temperature Effects on Biaxial Fatigue of 304 SS

However, this approach is not valid if one examines Figure (6) where the temperature environment is 1200°F. The data does not follow the room temperature observation despite the fact that an upper bound is still the torsional data. The 1200°F environment shows a considerable detrimental factor on the life of the material under biaxial loading, since the biaxial test data falls below the axial data (a lower bound at room temperature). The most critical scatter and deteriorating in life takes place at $N \leq 10^3$ cycles. This behavior is not noticeable at 1000°F shown in Figure (7). The life at 1000°F was reduced by a factor of 4 while at 1200°F by a factor of 10. It is suspected that at 1200°F, a drastic drop in the mechanical properties of 304 SS takes place.

It is also observed that two life regions have developed at 1200°F with 10^3 cycles as a transition mode. Although no definite explanation can be forwarded for this transition at this time, attention should be drawn to the left side region where to some extent the slope of the line is the same as that drawn for room and 1000°F data lines. Also the reduction in life is severe when compared to room temperature. To check this observed transition region and to determine the effect of temperature range on the mechanical properties of the material tested in biaxial fatigue, monotonic tension tests at 1000°F, 1100°F and 1200°F were conducted.

2. Biaxial Cumulative Fatigue Damage Tests

Biaxial cumulative fatigue damage tests were conducted under a high load followed by a low load sequence. The aim of the cumulative fatigue damage tests is to predict the service life of structural components under such load-

ing conditions based on the conventional σ-N diagrams. The linear damage rule utilized in design procedures is used in the analysis of the test results. It hypothesizes that the fraction of damage created by the cycles n_i applied at the i^{th} stress level of a loading sequence is given by the cycle ratio $\frac{n_i}{N_i}$, where N_i is the number of cycles necessary to cause fatigue failure at the i^{th} stress level of the loading sequence. When the total damage is equal to 1, fatigue failure is predicted. Therefore, based on this criterion and its assumption, tests have been conducted at room temperature to serve as a guideline and base data for the evaluation of high temperature effect. Six tests were conducted under a biaxiality ratio of 2. The biaxiality ratio consists of shear strain range to axial strain range imposed in the loading sequence shown in Figure (8). A typical biaxial cumulative damage test procedure is presented in Table (3). The initial step consists of a biaxial cyclic ratio that varied from 10% to 89.4%, followed by a final step to complete failure. The step down procedure shows the effect of loading sequence with respect to the "Miner" Linear Damage Rule. Table (4) shows the results of six tests at room temperature and seven tests at 1200°F. The percentage distribution of the high-load life which was applied first is plotted against the value of "Miner" cumulative addition. This type of representation is shown in Figure (9). It can be observed from the data presented in Figure (9) that 10% duration is greater than 1. However, when the percentage is increased to 20% and more, the value of "Miner" cumulative damage falls below 1 and continues in the same fashion till 90%, after which the tendency is to regain its original value of 1. This change in behavior for values of less than 20% and greater than 90% is represented by a dashed line, showing the discrepancy that takes

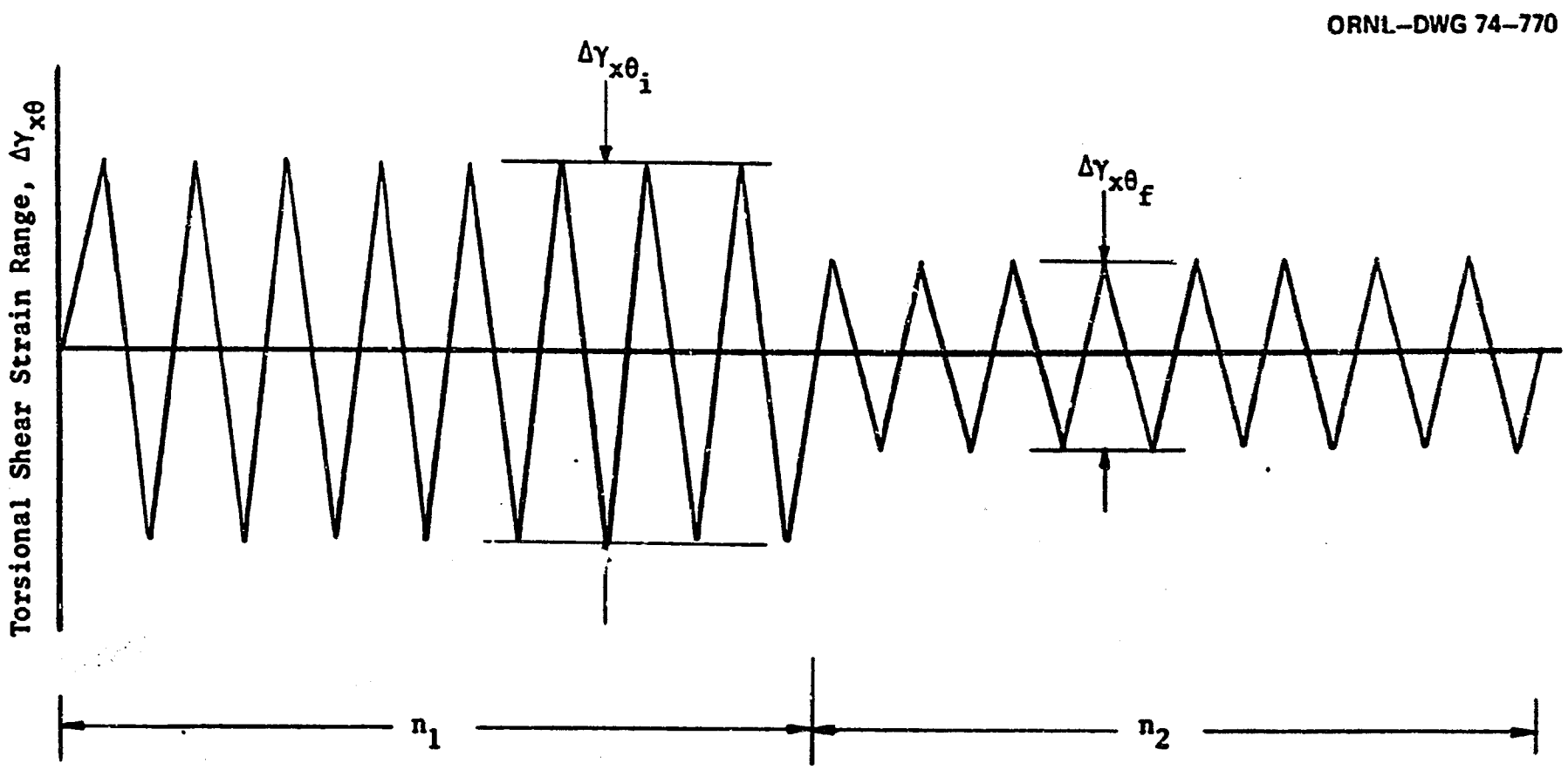

Fig. 8. Loading sequence for biaxial cumulative fatigue damage tests. Subscripts i and f represent initial and final step respectively.

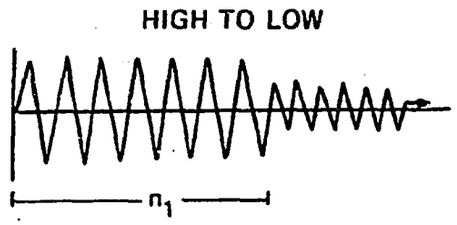

Fig. 9. Miner's rule in biaxial cumulative fatigue damage for tubular specimens of 304 stainless steel (heat 9T2796) at room temperature.

place within that region and which has to be explored further. It is possible to speculate that crack initiation and its propagating mode has a significant influence on this observed behavior.

Biaxial cumulative damage tests under 1200°F and 1000°F are in progress. The tests are carried out in the same procedure that was outlined in Table (3).

3. Tensile Properties of 304 Stainless Steel

Tensile tests were conducted on five specimens; one at room temperature and four at temperatures ranging from 900°F to 1200°F. The mechanical properties determined from these tensile tests are presented in Table (5). The temperature range of 1200°F shows the most significant effect on the strength characteristic of the material tested. For example, the measured ultimate strength at room temperature is 78 ksi, whereas, at 1200°F it is reduced to 36 ksi. Similarly, a 40% reduction in area was observed. Figure (10) shows the calculated stress-strain diagram in the plastic region. The elastic region was measured on a different deformation scale. The yield stress was calculated using the 0.2% offset method. The changes in the mechanical properties as a result of the applied temperatures are shown in Figures (11) through (11D). It should be noted that the tensile tests were conducted on hollow round specimens of the same thickness as those used in fatigue tests. Figure (12) shows the high temperature tensile machine.

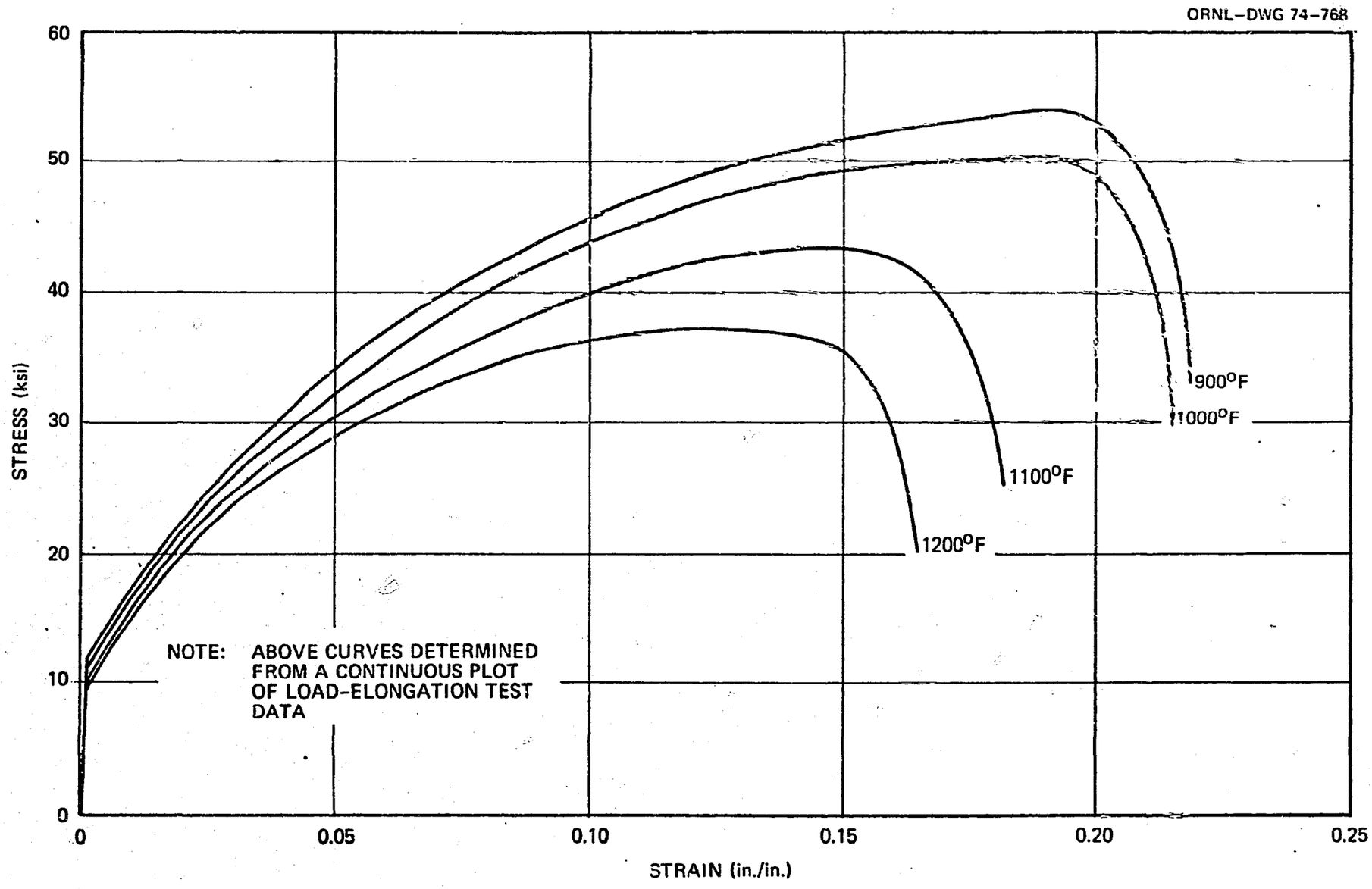

Fig. 10. Tensile properties as function of temperature for tubular specimens of 304 stainless steel (heat 9T2796).

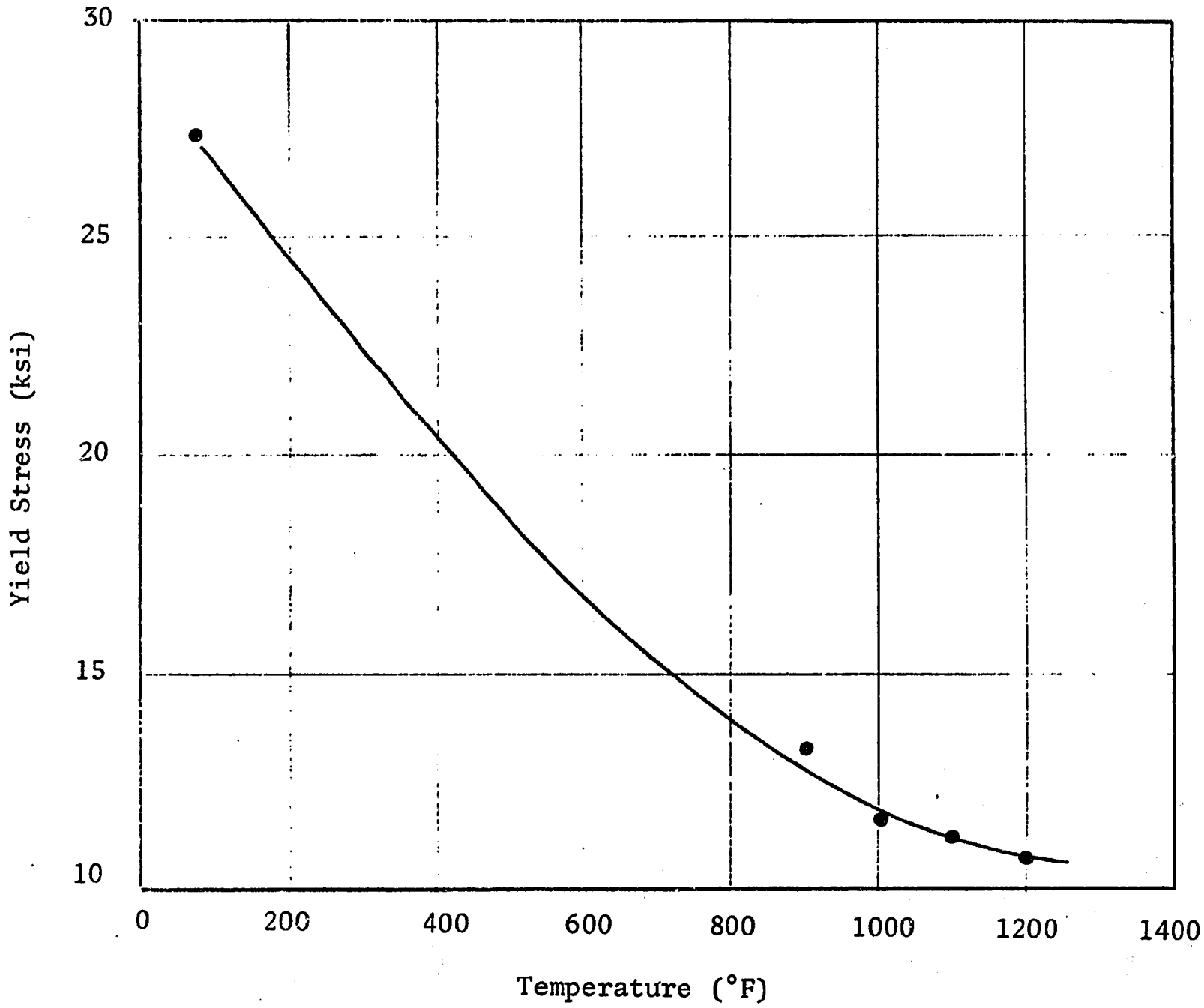

Figure 11 - Yield stress vs temperature for tubular specimens of 304 stainless steel (heat 9T2796)

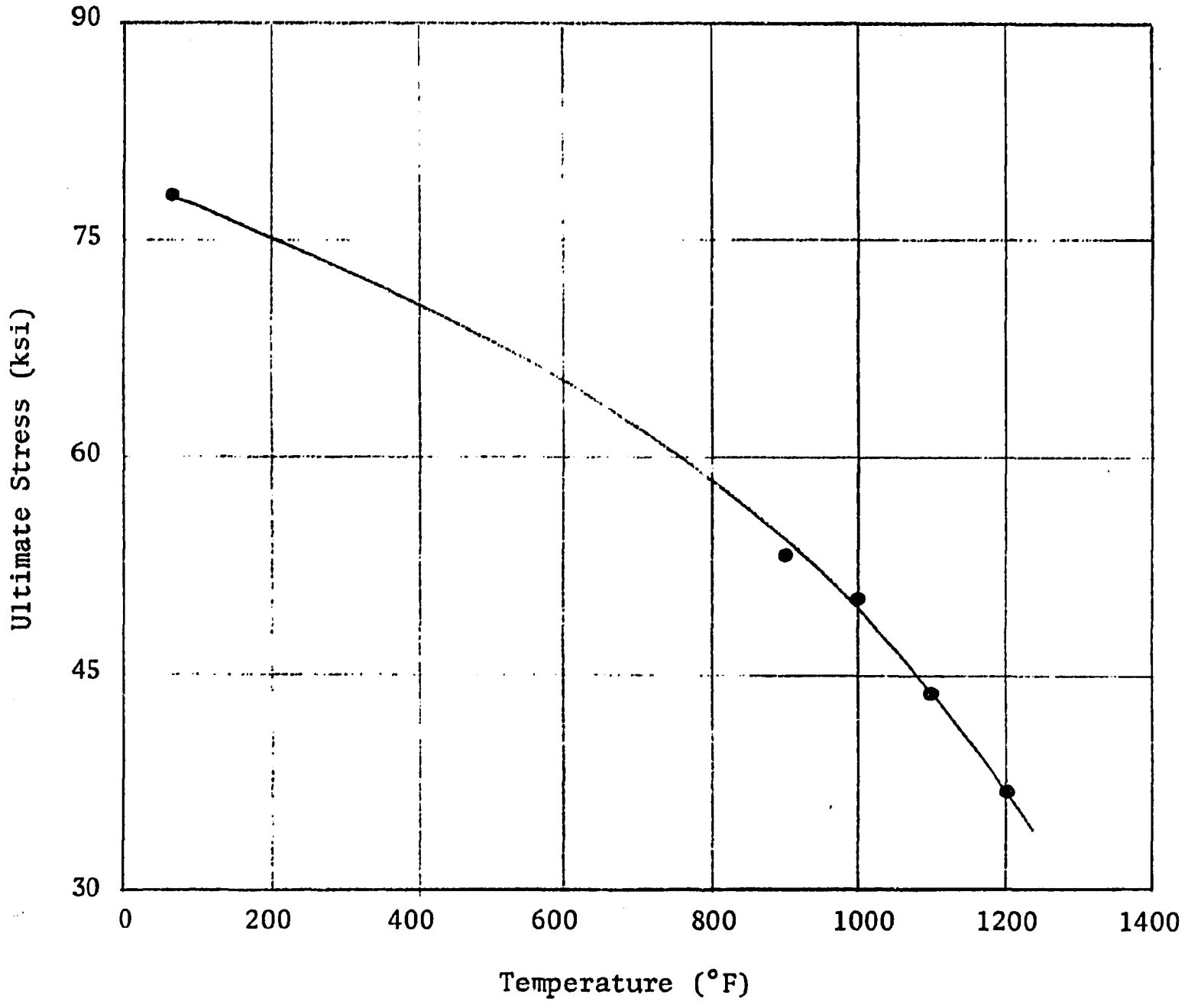

Figure 11A - Ultimate stress vs temperature for tubular specimens of 304 stainless steel (heat 9T2796)

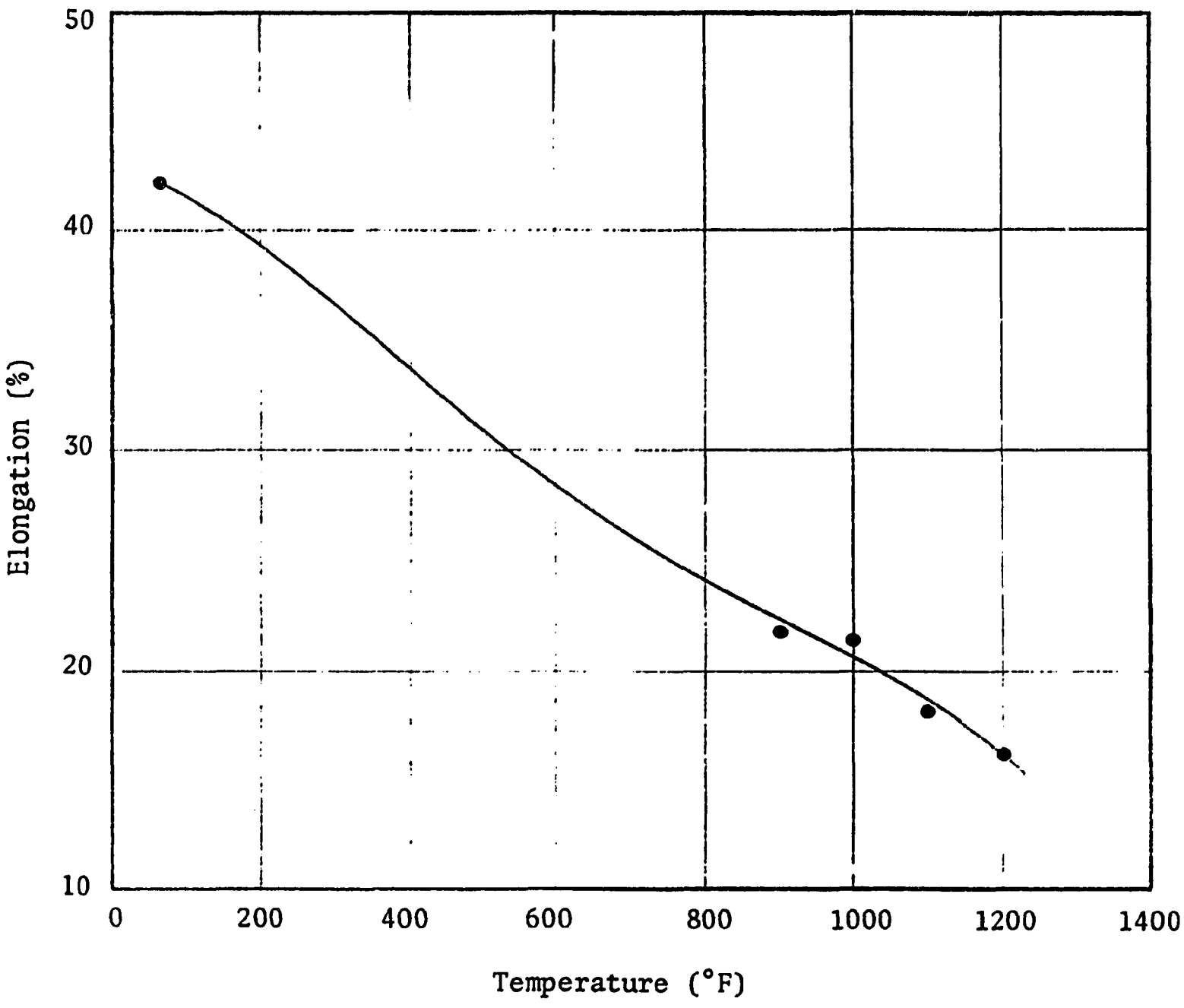

Figure 11B - Elongation vs temperature for tubular specimens of 304 stainless steel (heat 9T2796)

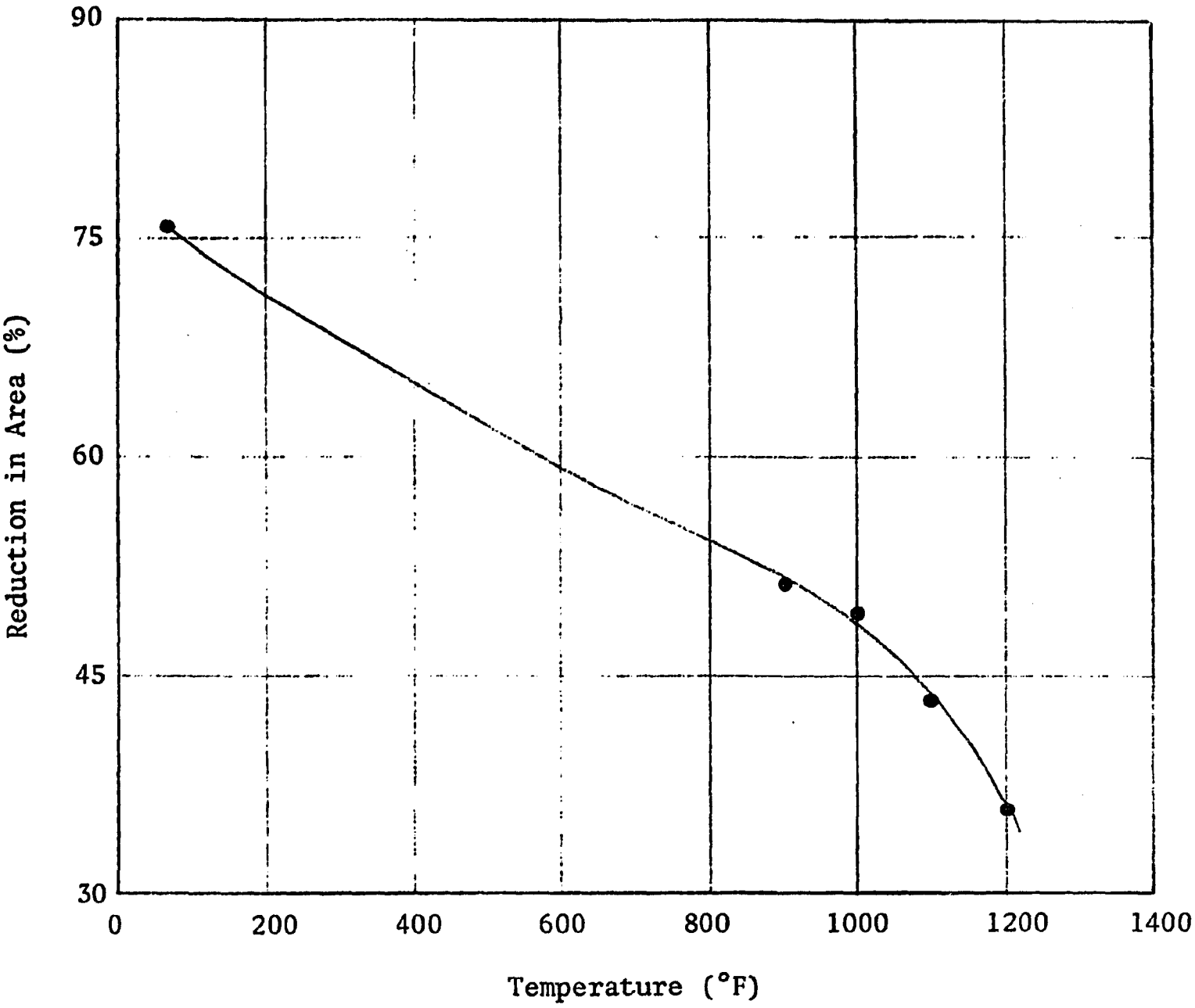

Figure 11C - Reduction in area vs temperature for tubular specimens of 304 stainless steel (heat 9T2796)

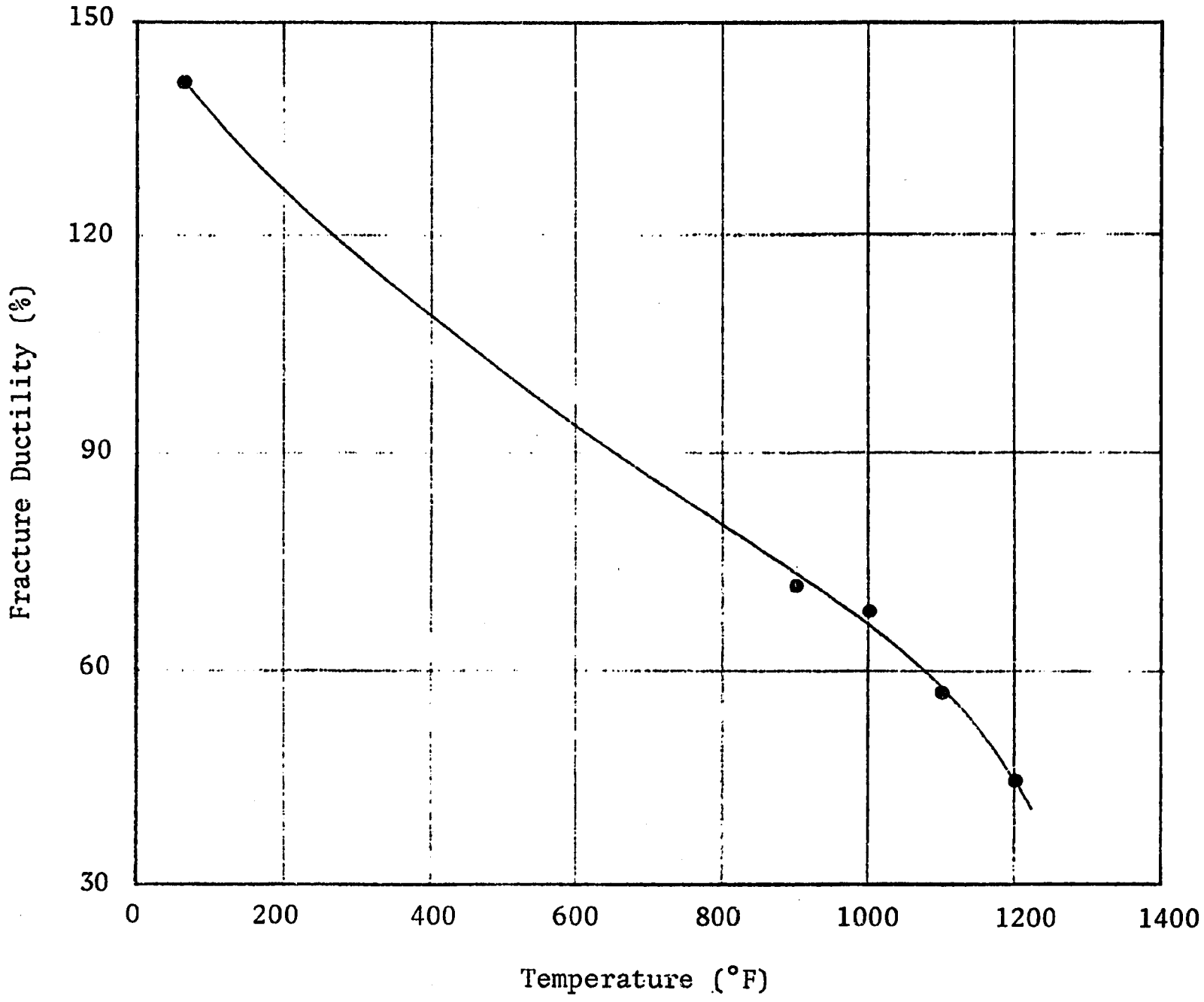

Figure 11D - Fracture ductility vs temperature for tubular specimens of 304 stainless steel (heat 9T2796)

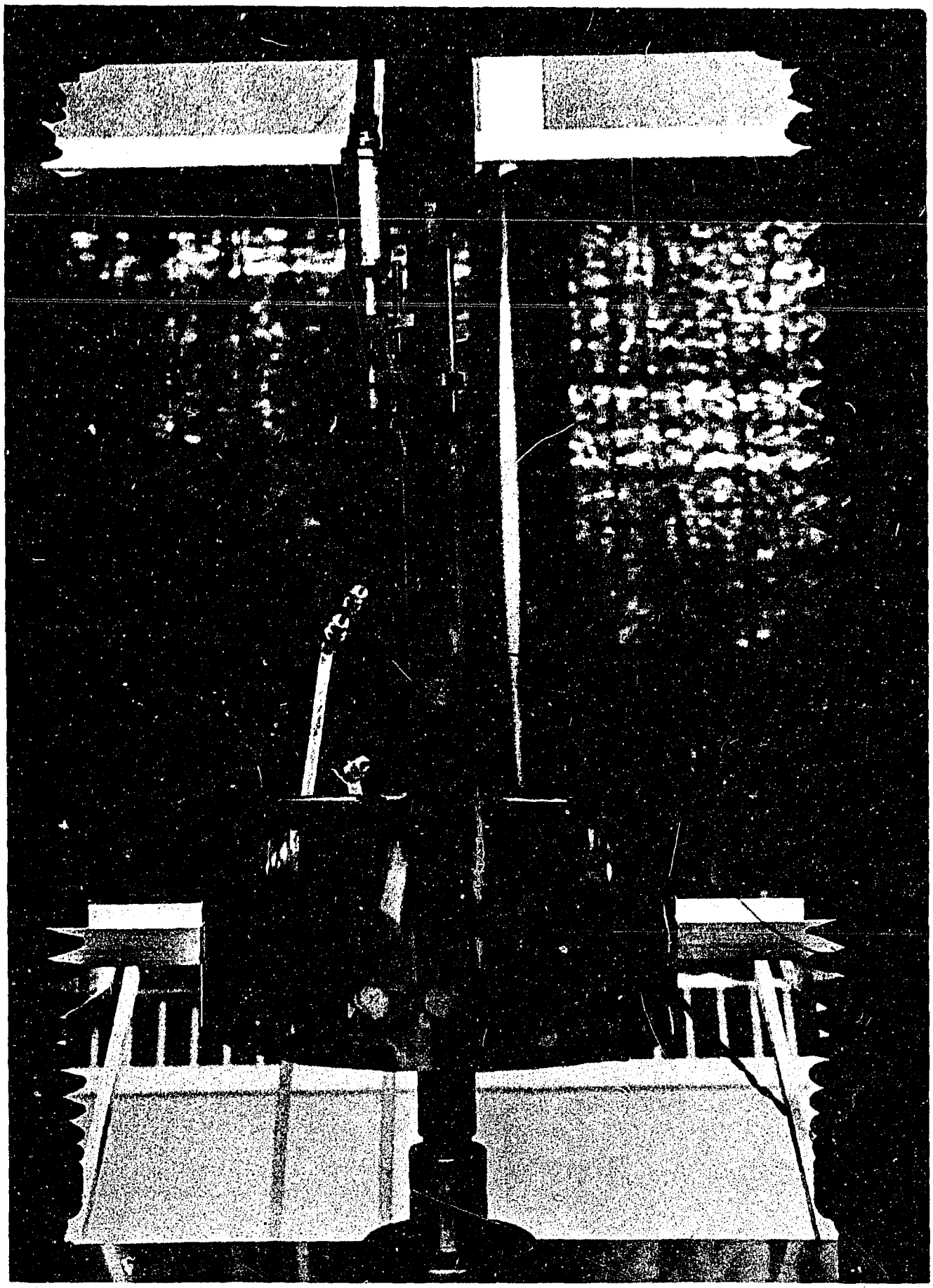

Figure 12 - High Temperature Tensile Test Machine

Table 1 Biaxial fatigue test results for 304 stainless steel (heat 9T2796)

Specimen No.	Axial Strain Range $\Delta\varepsilon_x$ (%)	Torsional Shear Strain Range $\Delta\gamma_{x\theta}$ (%)	$\frac{\Delta\gamma_{x\theta}}{\Delta\varepsilon_x}$ (R)	Temp. (°F)	Principal Strain Ranges $\Delta\varepsilon_1$ (%)	$\Delta\varepsilon_2$ (%)	$\Delta\varepsilon_3$ (%)	Total Strain Range $\Delta\varepsilon_T$ (%)	Effective Strain Range $\Delta\varepsilon_e$ (%)	Octahedral Shear Strain Range $\Delta\gamma_{oct}$ (%)	# of Cycles To Failure (N)
G 14	2.00	1.00	0.5	Room	2.08	-1.08	-1.00	2.55	2.08	2.94	1075
G 17	1.50	0.75	0.5	Room	1.56	-0.81	-0.75	1.91	1.56	2.21	1700
G 18	0.50	0.25	0.5	Room	0.52	-0.27	-0.25	0.64	0.52	0.74	11550
G 15	2.00	2.00	1.0	Room	2.30	-1.30	-1.00	2.82	2.30	3.26	1160
G 20	0.80	0.80	1.0	Room	0.921	-0.521	-0.40	1.13	0.92	1.30	4100
H 1	1.00	2.00	2.0	Room	1.50	-1.00	-0.50	1.87	1.53	2.16	2780
H 2	0.75	1.50	2.0	Room	1.125	-0.75	-0.375	1.40	1.14	1.62	4300
H 3	0.60	1.20	2.0	Room	0.90	-0.60	-0.30	1.12	0.91	1.30	6000
H 4	0.50	1.00	2.0	Room	0.75	-0.50	-0.25	0.94	0.77	1.08	6900
G 16	1.00	5.00	5.0	Room	2.86	-2.36	-0.50	3.74	3.05	4.32	1100
H 6	0.50	0.25	0.5	1200	0.52	-0.27	-0.25	0.64	0.52	0.74	2452
H 7	1.50	0.75	0.5	1200	1.56	-0.81	-0.75	1.91	1.56	2.21	150
I 6	0.80	0.40	0.5	1200	0.832	-0.432	-0.40	1.02	0.83	1.17	164
H 18	1.20	0.60	0.5	1200	1.248	-0.648	-0.60	1.53	1.25	1.77	110
H 16	0.60	0.30	0.5	1200	0.62	-0.32	-0.30	1.12	0.62	0.88	1074
I 3	0.72	0.72	1.0	1200	0.83	-0.47	-0.36	1.02	0.83	1.18	100
I 2	0.60	0.60	1.0	1200	0.69	-0.39	-0.30	0.847	0.69	0.98	700
I 4	0.90	0.90	1.0	1200	1.04	-0.59	-0.45	1.133	1.04	1.47	152
I 5	0.40	0.40	1.0	1200	0.46	-0.26	-0.20	0.565	0.46	0.65	1121
I 15	0.40	0.40	1.0	1200	0.46	-0.26	-0.20	0.565	0.46	0.65	2390
I 16	0.70	0.70	1.0	1200	0.81	-0.46	-0.35	0.995	0.81	1.15	865
H 8	0.60	1.20	2.0	1200	0.90	-0.60	-0.30	1.12	0.91	1.30	693
H 9	0.75	1.50	2.0	1200	1.125	-0.75	-0.375	1.40	1.14	1.63	400
H 11	0.50	1.00	2.0	1200	0.75	-0.50	-0.25	0.94	0.77	1.08	830
H 13	0.30	0.60	2.0	1200	0.45	-0.30	-0.15	0.56	0.46	0.65	4045
H 14	0.40	0.80	2.0	1200	0.60	-0.40	-0.20	0.75	0.61	0.86	2612
H 15	0.60	1.20	2.0	1200	0.90	-0.60	-0.30	1.12	0.91	1.30	800
H 19	0.28	0.56	2.0	1200	0.42	-0.28	-0.14	0.52	0.43	0.60	7800
H 17	0.25	0.50	2.0	1200	0.375	-0.25	-0.125	0.47	0.39	0.55	12800
I 7	0.2	1.00	5.0	1200	0.572	-0.472	-0.10	0.748	0.61	0.86	6200
I 8	0.6	3.00	5.0	1200	1.716	-1.416	-0.30	2.24	1.83	2.59	215
I 13	1.2	0.60	0.5	1000	1.248	-0.648	-0.60	1.529	1.248	1.764	1187
I 14	1.6	0.80	0.5	1000	1.664	-0.864	-0.80	2.039	1.664	2.353	680
I 9	0.8	0.80	1.0	1000	0.921	-0.521	-0.40	1.131	0.923	1.31	1698
I 10	0.6	0.60	1.0	1000	0.691	-0.391	-0.30	0.848	0.692	0.978	3178
I 11	1.2	1.20	1.0	1000	1.381	-0.781	-0.60	1.697	1.385	1.958	835
I 12	1.0	1.00	1.0	1000	1.151	-0.651	-0.50	1.414	1.154	1.632	955

Table 2 - Biaxial Ratio Effect on the Calculated Yield Criteria

$R = \frac{\Delta\gamma_{x\theta}}{\Delta\varepsilon_x}$	$\phi = \frac{\Delta\varepsilon_2}{\Delta\varepsilon_1}$	Effective strain range $\Delta\bar{\varepsilon}_e$	Total strain range $\Delta\varepsilon_T$ [a]	Octahedral shear strain range $\Delta\gamma_{oct}$
0 (uniaxial)	−0.500	1.0000 $\Delta\varepsilon_1$	1.2247 $\Delta\varepsilon_1$	1.4142 $\Delta\varepsilon_1$
0.5	−0.5194	1.0002 $\Delta\varepsilon_1$	1.2251 $\Delta\varepsilon_1$	1.4145 $\Delta\varepsilon_1$
1.0	−0.5657	1.0028 $\Delta\varepsilon_1$	1.2283 $\Delta\varepsilon_1$	1.4182 $\Delta\varepsilon_1$
2	−0.6666	1.0181 $\Delta\varepsilon_1$	1.2469 $\Delta\varepsilon_1$	1.4399 $\Delta\varepsilon_1$
3	−0.74053	1.0378 $\Delta\varepsilon_1$	1.2710 $\Delta\varepsilon_1$	1.4677 $\Delta\varepsilon_1$
4	−0.7904	1.0547 $\Delta\varepsilon_1$	1.2917 $\Delta\varepsilon_1$	1.4916 $\Delta\varepsilon_1$
5	−0.8252	1.0681 $\Delta\varepsilon_1$	1.3082 $\Delta\varepsilon_1$	1.5105 $\Delta\varepsilon_1$
6	−0.8504	1.0787 $\Delta\varepsilon_1$	1.3211 $\Delta\varepsilon_1$	1.5255 $\Delta\varepsilon_1$
7	−0.8694	1.0871 $\Delta\varepsilon_1$	1.3314 $\Delta\varepsilon_1$	1.5374 $\Delta\varepsilon_1$
8	−0.8842	1.0940 $\Delta\varepsilon_1$	1.3399 $\Delta\varepsilon_1$	1.5471 $\Delta\varepsilon_1$
9	−0.8961	1.0996 $\Delta\varepsilon_1$	1.3467 $\Delta\varepsilon_1$	1.5550 $\Delta\varepsilon_1$
10	−0.9057	1.1043 $\Delta\varepsilon_1$	1.3525 $\Delta\varepsilon_1$	1.5617 $\Delta\varepsilon_1$
∞ (pure torsion)	−1.0000	1.1547 $\Delta\varepsilon_1$	1.4142 $\Delta\varepsilon_1$	1.6330 $\Delta\varepsilon_1$

[a] $\Delta\varepsilon_T = \sqrt{2}\,\Delta\varepsilon_1[1 + \phi + \phi^2]^{1/2}$

TABLE 3 - Typical Cumulative Damage Test Procedure

Test Temperature (°F)	Biaxiality Ratio $R = \frac{\Delta\gamma_{x\theta}}{\Delta\varepsilon_x}$	Initial Step: Applied Axial Strain Range $\Delta\varepsilon_{x_i}$ (%)	Initial Step: Applied Torsional Shear Strain Range $\Delta\gamma_{x\theta_i}$ (%)	Initial Step: Number of Cycles to Failure at This Load Level N_1	Initial Step: Calculated Maximum Principal Strain Range $\Delta\varepsilon_1$ (%)	Initial Step: Calculated Octahedral Shear Strain Range $\Delta\gamma_{oct}$ (%)	Final Step $\Delta\varepsilon_{x_f}$ (%)	Final Step $\Delta\gamma_{x\theta_f}$ (%)	Final Step N_2 Cycles	Final Step $\Delta\varepsilon_1$ (%)	Final Step $\Delta\gamma_{oct}$ (%)
Room	2	1.00	2.00	2780	1.50	2.16	0.50	1.00	9000	0.75	1.08
1200°	2	1.00	2.00	300	1.50	2.16	0.50	1.00	1000	0.75	1.08

Table 4. Biaxial cumulative fatigue damage test for specimens of type 304 stainless steel heat 9T2796

Specimen No.	Test temperature [°C (°F)]	Biaxiality ratio, $R = \frac{\Delta\gamma_{x\theta}}{\Delta\varepsilon_x}$	Initial step			Final step			$\Sigma \frac{n_i}{N_i}$
			N_1 cycles	n_1 cycles	$\frac{n_1}{N_1}$ (%)	N_2 cycles	n_2 cycles	$\frac{n_2}{N_2}$	
I.17	Room	2	2780	278	10.0	9000	12,500	1.388	1.488
I.21	Room	2	2780	556	20.0	9000	7,040	0.782	0.982
I.18	Room	2	2780	1112	40.0	9000	5,038	0.560	0.960
I.19	Room	2	2780	1668	60.0	9000	2,962	0.330	0.930
I.20	Room	2	2780	2224	80.0	9000	760	0.080	0.880
J.1[a]	Room	2	2780	2484[b]	89.4	9000			0.894
J.2	649 (1200)	2	300	30	10.0	1000	1,385	1.385	1.485
J.12	649 (1200)	2	300	60	20	1000	728	0.728	0.928
J.10	649 (1200)	2	300	120	40	1000	492	0.492	0.892
J.9	649 (1200)	2	300	180	60	1000	241	0.241	0.841
J.8	649 (1200)	2	300	210	70	1000	110	0.110	0.810
J.6	649 (1200)	2	300	240	80	1000	48	0.048	0.848
J.7	649 (1200)	2	300	270	90	1000	20	0.020	0.920

[a] Bar 38.

[b] Specimen fractured before low load level applied.

Table 5. Summary of tensile tests on tubular specimens[a] taken from nominal 1.0-in.-diam bar of type 304 stainless steel (heat 9T2796)

Specimen No.	Test temperature [°C (°F)]	Strain rate (min^{-1})	0.2% yield (psi)	Ultimate strength (psi)	Elongation in 2.375 in. (%)	Reduction in area[b] (%)	Fracture ductility[c] (%)
C.1	Room	0.0421	27,362.28	78,112.28	42.105	75.61	141.099
C.5	482 (900)	0.0421	13,179.66	53,609.75	21.852	51.19	71.686
C.3	538 (1000)	0.0421	11,547.64	50,188.09	21.347	49.39	68.310
C.7	593 (1100)	0.0421	11,175.56	43,412.75	18.274	43.22	56.531
C.6	649 (1200)	0.0421	10,686.22	36,733.86	16.295	35.68	44.469

[a] All specimens were annealed at 2000°F for 0.5 hr in an argon atmosphere.

[b] Reduction in area: $RA = \frac{A_i - A_f}{A_i}$, where A_i is initial area and A_f is final area.

[c] Fracture ductility: $FD = \ln \frac{1}{1 - RA}$.

Table 6. Chart giving numbers and dimensions of specimens taken from 1-in. diam bar type 304 stainless steel (heat 9T2796)

Specimen number[a]	Inside diameter	Outside diameter
I 1	0.337 in.	0.457 in.
I 2	0.336 in.	0.456 in.
I 3	0.339 in.	0.459 in.
I 4	0.340 in.	0.460 in.
I 5	0.344 in.	0.464 in.
I 6	0.340 in.	0.460 in.
I 7	0.342 in.	0.462 in.
I 8	0.342 in.	0.462 in.
I 9	0.342 in.	0.462 in.
I 10	0.340 in.	0.460 in.
I 11	0.345 in.	0.465 in.
I 12	0.346 in.	0.466 in.
I 13	0.347 in.	0.467 in.
I 14	0.346 in.	0.466 in.
I 15	0.348 in.	0.468 in.
I 16	0.347 in.	0.467 in.
I 17	0.343 in.	0.463 in.
I 18	0.349 in.	0.469 in.
I 19	0.344 in.	0.464 in.
I 20	0.342 in.	0.462 in.
I 21	0.347 in.	0.467 in.

[a]The letter I refers to specimens taken from bar No. 35.

Table 6A. Numbers and dimensions of specimens taken from 1-in.-diam bar type 304 stainless steel (heat 9T2796)

Specimen No.	Inside diameter (in.)	Outside diameter (in.)
C.1	0.347	0.467
C.2	0.349	0.469
C.3	0.338	0.458
C.4	0.335	0.455
C.5	0.337	0.457
C.6	0.337	0.457
C.7	0.337	0.457
C.8	0.339	0.459
C.9	0.338	0.458
C.10	0.338	0.458
J.1[a]	0.344	0.464
J.2	0.347	0.467
J.3	0.348	0.468
J.4	0.343	0.463
J.5	0.345	0.465
J.6	0.346	0.466
J.7	0.345	0.465
J.8	0.347	0.467
J.9	0.346	0.466
J.10	0.348	0.468
J.11	0.345	0.465
J.12	0.345	0.465
J.13	0.346	0.466
J.14	0.345	0.465
J.15	0.344	0.464
J.16	0.342	0.462
J.17	0.341	0.461
J.18	0.342	0.462
J.19	0.347	0.467
J.20	0.344	0.464
J.21	0.341	0.461
J.22	0.347	0.467

[a]Bar 38.